doi:10.1093/brain/awp076 Brain 2009: 132; 1480–1495 | 1480

BRAIN
A JOURNAL OF NEUROLOGY

Selective adenosine A_{2a} receptor antagonism reduces JNK activation in oligodendrocytes after cerebral ischaemia

Alessia Melani,[1,2] Sara Cipriani,[1] Maria Giuliana Vannucchi,[3] Daniele Nosi,[3] Chiara Donati,[4] Paola Bruni,[4] Maria Grazia Giovannini[1] and Felicita Pedata[1]

1 Department of Preclinical and Clinical Pharmacology, University of Florence, Florence, Italy
2 IRCCS Centro Neurolesi 'Bonino-Pulejo', Messina, Italy
3 Department of Anatomy, Histology and Forensic Medicine, University of Florence, Florence, Italy
4 Department of Biochemical Sciences, University of Florence, Florence, Italy

Correspondence to: Prof. Felicita Pedata,
Department of Preclinical and Clinical Pharmacology,
University of Florence,
Viale Pieraccini,
6, 50139 Florence, Italy
E-mail: felicita.pedata@unifi.it

Adenosine is a potent biological mediator, the concentration of which increases dramatically following brain ischaemia. During ischaemia, adenosine is in a concentration range (μM) that stimulates all four adenosine receptor subtypes (A_1, A_{2A}, A_{2B} and A_3). In recent years, evidence has indicated that the A_{2A} receptor subtype is of critical importance in stroke. We have previously shown that 24 h after medial cerebral artery occlusion (MCAo), A_{2A} receptors up-regulate on neurons and microglia of ischaemic striatum and cortex and that subchronically administered adenosine A_{2A} receptor antagonists protect against brain damage and neurological deficit and reduce activation of p38 mitogen-activated protein kinase (MAPK) in microglial cells. The mechanisms by which A_{2A} receptors are noxious during ischaemia still remain elusive. The objective of the present study was to investigate whether the adenosine A_{2A} antagonist SCH58261 affects JNK and MEK1/ERK MAPK activation. A further aim was to investigate cell types expressing activated JNK and MEK1/ERK MAPK after ischaemia. We hereby report that the selective adenosine A_{2A} receptor antagonist, SCH58261, administered subchronically (0.01 mg/kg i.p) 5 min, 6 and 20 h after MCAo in male Wistar rats, reduced JNK MAPK activation (immunoblot analysis: phospho-JNK54 isoform by 81% and phospho-JNK46 isoform by 60%) in the ischaemic striatum. Twenty-four hours after MCAo, the Olig2 transcription factor of oligodendroglial progenitor cells and mature oligodendrocytes was highly expressed in cell bodies in the ischaemic striatum. Immunofluorescence staining showed that JNK MAPK is maximally expressed in Olig2-stained oligodendrocytes and in a few NeuN stained neurons. Striatal cell fractioning into nuclear and extra-nuclear fractions demonstrated the presence of Olig2 transcription factor and JNK MAPK in both fractions. The A_{2A} antagonist reduced striatal Olig 2 transcription factor (immunoblot analysis: by 55%) and prevented myelin disorganization, assessed by myelin-associated glycoprotein staining. Twenty-four hours after MCAo, ERK1/2 MAPK was highly activated in the ischaemic striatum, mostly in microglia, while it was reduced in the ischaemic cortex. The A_{2A} antagonist did not affect activation of the ERK1/2 pathway. The efficacy of A_{2A} receptor antagonism in reducing activation of JNK MAPK in oligodendrocytes suggests a mechanism of protection consisting of scarring oligodendrocyte inhibitory molecules that can hinder myelin reconstitution and neuron functionality.

Keywords: oligodendrocytes; Olig2; JNK MAPK; ERK1/2 MAPK; adenosine A_{2A} receptor antagonist

Received August 7, 2008. Revised February 9, 2009. Accepted February 20, 2009. Advance Access publication April 9, 2009

Introduction

Adenosine is a potent biological mediator which increases dramatically in concentration following brain ischaemia (Melani *et al*., 1999, 2003; Phillis, 2004). During ischaemia, extra-cellular adenosine is in a concentration range (μM) that stimulates all four adenosine receptor subtypes (A_1, A_{2A}, A_{2B} and A_3). In recent years, evidence has shown that the A_{2A} receptor subtype is of critical importance in stroke (Chen *et al*., 2007). Genetic deletion of A_{2A} receptors reduces ischaemic and functional damage in a mouse model, where focal ischaemia is induced by medial cerebral artery occlusion (MCAo) (Chen *et al*., 1999). In the same model, we have recently reported an up-regulation of A_{2A} adenosine receptors on neurons and microglia of ischaemic striatum and cortex (Trincavelli *et al*., 2008). After MCAo, selective A_{2A} receptor antagonists reduce ischaemic brain damage and neurological deficit (Monopoli *et al*., 1998*b*; Melani *et al*., 2003, 2006). All evidence suggests a noxious role of adenosine A_{2A} receptors in brain ischaemia. The intimate mechanisms by which A_{2A} receptors are noxious in ischaemia still remain elusive and must be clarified.

A_{2A} receptors are expressed at high levels in the corpus striatum, nucleus accumbens and olfactory tubercles and to a lesser extent in the cortex (Rosin *et al*., 1998). A_{2A}-receptor mRNA has been found in neurons (Schiffmann *et al*., 1991; Fink *et al*., 1992), in microglia (Fiebich *et al*., 1996) and in oligodendrocytes (Stevens *et al*., 2002), while controversial data on its presence in astrocytes have been reported (Fiebich *et al*., 1996; Nishizaki *et al*., 2002; Brambilla *et al*., 2003; Lee *et al*., 2003; Wittendorp *et al*., 2004). Evidence indicates that the A_{2A} receptor stimulates glutamate outflow from neurons and glial cells (Chen and Pedata, 2008). A_{2A} receptor antagonists, in turn, reduce glutamate outflow in the MCAo model in the rat (Melani *et al*., 2003). Therefore, A_{2A} receptors present on neurons or glial cells may exert a deleterious effect by increasing early excitotoxicity after ischaemia. We have demonstrated that repeated administration of the selective A_{2A} receptor antagonist, SCH 58261, reduces activation of p38 mitogen-activated protein kinase (MAPK) in microglial cells (Melani *et al*., 2006). Recent studies suggest that inflammation mediated by microglia plays a role in neurodegeneration. This suggests that A_{2A} receptors are also involved in regulating factors responsible for the delayed detrimental inflammatory effects in brain ischaemia. Activation of p38 and JNK MAPKs is well documented in focal cerebral ischaemia models (Irving *et al*., 2000; Melani *et al*., 2006). Modification of phospho-ERK1/2 MAPK has been reported at different times after focal cerebral ischaemia models both in neurons and glial cells (Irving *et al*., 2000; Wu *et al*., 2000; Borsello *et al*., 2003; Wang *et al*., 2003). MAPKs are essential in regulating cell growth, survival, differentiation and death (Irving and Bamford, 2002). The cell type in which MAPKs are activated is relevant to the understanding of death or survival mechanisms in ischaemia.

Several agents preventing the activation of JNK or c-Jun phosphorylation have been shown to protect the brain after cerebral ischaemia (Repici and Borsello, 2006). The protease-resistant cell-penetrating peptide D-JNK administered i.c.v. (Borsello *et al*., 2003) or i.v (Esneault *et al*., 2008) between 3 h and 6 h after transient ischaemia in adult mice and rats, improves motor performance and cognitive functions. In the MCAo model, inhibition of the MEK1/ERK pathway protects the brain from ischaemic injury, reducing both brain damage, neurological deficit (Alessandrini *et al*., 1999; Namura *et al*., 2001; Wang *et al*., 2003) and IL-1beta expression (Wang *et al*., 2004).

In the present study, we evaluated the capacity of the selective A_{2A} receptor antagonist, SCH 58261 subchronically administered i.p. after permanent focal ischaemia, to modulate JNK and ERK1/2 MAPKs activation after permanent MCAo. Twenty-four hours after MCAo, the A_{2A} antagonist did not affect ERK1/2 activation but substantially reduced JNK activation. Reduced JNK phosphorylation occurs predominantly in oligodendrocytes and might account for A_{2A} antagonist-protection from ischaemic damage.

Materials and Methods

Animal housing and surgery

Male Wistar rats (Harlan, Italy) weighing 270–290 g were used. They were housed in groups of three with free access to food and water and kept on a 12 h light/dark cycle. The animals were kept under standardized temperature, humidity and light conditions with free access to food and water.

Animal care and use followed the directives of the Council of the European Community (86/609/EC). All efforts were made to minimize animal suffering and to reduce the number of animals used.

Focal cerebral ischaemia was induced by permanent MCAo in the right hemisphere. The animals were anaesthetized with 5.0% isoflurane (Baxter International) and spontaneously inhaled 1.0–2.0% isoflurane in air by the use of a mask. Body core temperature was maintained at 37°C with a recirculating pad and K module and was monitored via an intrarectal type T thermocouple (Harvard, Kent, UK). The rats were placed in a stereotaxic frame (Kopf). The surgical procedure to occlude the MCA consisted of the insertion of a 4–0 nylon monofilament (Ethilon, Johnson & Johnson, Somerville, NJ, USA), precoated with silicone (Xantopren, Heraeus Kulzer, Germany) mixed with a hardener (Omnident, Germany), via the external carotid artery into the internal carotid artery to block the origin of the MCA according to the procedure originally described by Longa *et al*. (1989) and modified by Melani *et al*. (1999). The sham operation was conducted by inserting the filament into the internal carotid artery and immediately withdrawing it. At the end of the surgical procedure, anaesthesia was discontinued and the animals were returned to a prone position. Recovery from anaesthesia took 15 min, thereafter the animals were allowed free access to food and water.

SCH 58261 (Sigma-Aldrich, St. Louis, Missouri, USA) was dissolved by sonication in saline with 1% Tween 80. In the SCH 58261-treated ($n = 14$) and vehicle-treated ($n = 13$) rats, the drug or vehicle was administered intraperitoneally 5 min, 6 h and 20 h after occlusion, respectively. The SCH 58261 dose administered (0.01 mg/kg) was calculated on the basis of those found protective against ischaemia in previous *in vivo* studies (Monopoli *et al*., 1998*b*; Melani *et al*., 2003; Pedata *et al*., 2005). It is worth mentioning that SCH 58261 up to the dose of 1 mg/kg i.p. (Monopoli *et al*., 1998*a*) does not modify any of the rat's hemodynamics. Sham-operated rats ($n = 12$) did not receive any treatment.

Motor behaviour

About 1 h after MCAo rats showed spontaneous turning behaviour that was evaluated every 15 min for 3–4 h after MCAo, according to the procedure described by Melani *et al*. (2003). Motor activity was investigated in sham-operated, vehicle and drug-treated rats. After being placed in a round cage, the rat began rapid unidirectional walking along the perimeter of the cage and to chase its tail. The number of rotations was recorded manually. One rotation was computed when the rat completely circled the cage. Five separate counting periods of 3 min each, separated by 15 min intervals, were made. Values are reported as the mean rotation number during the five counting periods per hour. The same rats were also evaluated soon after awakening and 24 h later for failure to extend fully the left forepaw and for contralateral turning when pulled by the tail. Under this condition all rats showed a clear circling to the left side.

Neurological test

Neurological evaluation of motor sensory functions was carried out prior to and 24 h after MCAo. The examiners were blind as to the procedure that the rat had undergone. Evaluations were always performed between 10 and 11 am to exclude behavioural changes based on circadian rhythm. The neurological examination consisted of six tests (Garcia *et al*., 1995*b*; Melani *et al*., 2003): (i) spontaneous activity; (ii) symmetry in the movement of four limbs; (iii) forepaw outstretching; (iv) climbing; (v) body proprioception; and (vi) response to vibrissae touch. The score assigned to each rat at completion of the evaluation equalled the sum of all six test scores. The final minimum score was 3 and the maximum was 18.

Histological analysis

After evaluation of motor behaviour and neurological deficit, i.e. 24 h after MCAo, some of the vehicle-treated ($n = 5$), SCH 58261-treated ($n = 5$) and sham-operated rats ($n = 4$) were randomly chosen and analysed for ischaemic damage using the following histological method.

The rats were anaesthetized with chloral hydrate (i.p., Sigma-Aldrich, St. Louis, MI, USA) and sacrificed by decapitation. The brains were rapidly removed and fixed with Liquid of Carnoy (6:3:1 absolute ethanol, chloroform and glacial acetic acid) and then embedded in paraffin after dehydration in different concentrations of ethanol and xylol. Coronal sections (7–8 μm) were collected at 1-mm intervals at eight different levels through the striatum (from +2.2 Bregma to −4.8 Bregma, corresponding to the ischaemic area) and were stained with acetate cresyl violet (1%). The lesioned area of the brain was detected as a pale zone lacking the acetate cresyl violet staining reflecting mainly the extent of unlabelled necrotic neurons 24 h after MCAo (Garcia *et al*., 1995*a*). Tissue damage was found neither in the sham-operated rats nor in the hemisphere contralateral to the ischaemic side. Definite ischaemic tissue damage was found in the vascular territory supplied by the MCA i.e. the sensorimotor cortex and striatum.

The pallid area was measured utilizing an image analysis system (Image ProPlus, Image & Computer, Milan, Italy). Striatal and cortical damage was calculated in cubic milli metre.

Immunohistochemistry

After evaluation of motor behaviour and neurological deficit, i.e. 24 h after MCAo, some of the vehicle-treated ($n = 3$), SCH 58261-treated ($n = 3$) and sham-operated rats ($n = 3$) were randomly chosen and used for immunohistochemical studies.

The rats were perfused transcardially, under deep anaesthesia, with an ice-cold 4% paraformaldehyde solution (in phosphate buffer, pH 7.4). Brains were post-fixed overnight and cryoprotected in an 18% sucrose solution (in phosphate buffer) for at least 48 h.

Brains were cut with a cryostat and 30 μm-thick coronal sections were collected between +1.7 and −0.90 mm from bregma, therefore including almost the entire striatum area. Sections were placed in anti-freeze solution (30% ethylene glycol, 30% glycerol in phosphate buffer) and stored at –20°C until assay.

Phospho-JNK and phospho-ERK1/2 were detected using specific primary antibodies [1:500 phospho-SAPK/JNK MAPKase (Thr183/Tyr185) antibody; 1:500 phospho-p44/42 MAPKase (Thr/Tyr204) antibody; and Cell Signaling Technology].

Day 1: Coronal sections were mounted on gelatin-coated slides and processed for immunohistochemistry. The sections were washed with PBS-Triton X-100 0.3% (PBS-TX), incubated for 15 min in PBS-TX containing 0.75% H_2O_2, rinsed in PBS-TX and incubated at room temperature in blocking buffer (5 mg/ml albumin, 0.05% NaN_3 in PBSB-TX) for 60 min. After washing in PBS-TX, the sections were incubated overnight at 4°C with the polyclonal primary antibodies anti-phospho-JNK and anti-phospho-ERK1/2, dissolved in blocking buffer.

Day 2: The sections, rinsed three times in PBS-TX, were incubated for 1 h at room temperature, with the biotinylated secondary antibody anti-rabbit-IgG (1:333) dissolved in blocking buffer. After washing in PBS-TX, sections were incubated in avidin–biotin–peroxidase complex (ABC kit Elite standard, Vectastain, Vector Laboratories, Burlingame, CA, USA) for 60 min.

Finally, all sections were stained using diaminobenzidine (DAB-peroxidase, Vectastain, Vector) in the presence of NiCl.

All sections were examined using an Olympus BX40 microscope (Olympus, Milan, Italy) and photographed using a digital camera (Olympus DP50).

Confocal laser microscopy immunohistochemistry

To identify the cellular types that expressed phospho-JNK and phospho-ERK1/2 MAPKs, confocal laser microscopy, using a modification of the previously described method (Giovannini, 2002), was used on 30 μm-thick coronal sections cut and stored as described above.

Day 1. Coronal sections were mounted on gelatin-coated slides and washed in 0.1 M PBS-TX for 10 min, then blocked with blocking buffer for 40 min. Sections were then incubated, for 24 h at room temperature, with different antibodies: rabbit polyclonal antibodies, anti-phospho-JNK (phospho-SAPK/JNK, 1:500; Cell Signaling Technology), mouse monoclonal antibodies, anti-glial fibrillary acid protein (GFAP, 1:500; BD Biosciences Pharmingen, USA) used to visualize astrocytes, anti-Neuronal Nuclei (NeuN, 1:200 dilution; Chemicon, Temecula, CA, USA) used to visualize neurons, anti-myelin-associated glycoprotein (MAG, 1:250; Chemicon International) used to visualize myelinated processes of oligodendrocytes and OX-42 CD11b/c (1:200, BD Biosciences Pharmingen, USA), used to visualize microglia; and goat polyclonal antibody, anti-OLIG2 (N-17) (1:100; Santa Cruz Biotechnologies) used to visualize the cell body of oligodendrocytes.

Day 2. After washing in PBS-TX (three times, 10 min each), slices were incubated for 2 h at room temperature in the dark with fluorescein-conjugated goat anti-rabbit IgG and Texas red-conjugated

goat anti-mouse IgG (1:400; Vector Laboratories) or CY3-conjugated anti-goat IgG (1:500; Vector Laboratories) in Blocking buffer. After extensive washings, slices were mounted using Vectashield (Vectastain, Vector Laboratories) as a mounting medium and, after drying, were observed under an epifluorescent Zeiss Axioskop microscope and under a BioRad 1024 confocal laser scanning microscope (Cambridge, MA, USA) with laser beam excitation at 488 and 568 nm wavelength. —Fifteen to 20 optical sections were taken at 1.3 μm intervals, keeping all the parameters (pinhole, contrast and brightness) constant for slices from the same experiment. Images of 512 × 512 pixels were obtained, opened with Confocal Assistant 4.02 and image analysis was conducted on image *z*-stacks which contained the entire field of interest. Images were then digitally converted to green (phospho-JNK) and red (OLIG2, GFAP, NeuN, MAG, OX-42 CD11b/c). The images were then assembled into montages using Adobe Photoshop 7.0 (Adobe Systems, Mountain View, CA, USA).

Western blotting

After evaluation of motor behaviour and neurological deficit, i.e. 24 h after MCAo, some of the vehicle-treated ($n = 5$), SCH 58261-treated ($n = 5$) and sham-operated rats ($n = 5$) were randomly chosen and used for Western blot quantification of phospho-JNK and phospho-ERK1/2 MAPK.

Western immunoblotting was carried out as previously described (Giovannini *et al*., 2001). Rats were sacrificed 24 h after surgery. The right and left striata were microdissected and transferred to ice-cold microcentrifuge tubes, and kept at −80°C until assay. Care was taken to ensure that brain tissue remained frozen throughout the procedure. All Western analyses were performed blind to the experimental conditions. 20 μl of ice-cold RIPA buffer were added to each microgram of tissue and the samples were homogenized on ice directly into the Eppendorf tube. RIPA buffer had the following composition: Igepal 1:100; Na-deoxycholate 0.5%; 0.1% sodium dodecyl sulphate (SDS, Sigma, St. Louis, MO, USA); a protease inhibitor tablet (Sigma, St Louis, MO); 2 mM sodium pyrophosphate; 4 mM paranitrophenylphosphate; and 1 mM sodium ortovanadate. After homogenization, protein determination was performed in 4 μl for each sample using Bio-Rad Protein Assay reagent (Bio-Rad, Hercules, CA, USA). An appropriate volume of 6× loading buffer was added to the homogenates, and samples were boiled for 5 min. Samples (50 μg of proteins per well) were loaded onto a 10% SDS–PAGE gel and resolved by standard electrophoresis. The proteins were then transferred electrophoretically onto nitrocellulose membrane (Hybond-C extra; Amersham, Arlington Heights, IL, USA) using a transfer tank kept at 4°C, with typical parameters being O/N with a constant current of 10 mA. Membranes were blocked for 1 h at room temperature with blocking buffer (5% non-fat dry milk in Tris buffered saline, 0.1%TWEEN-20 and TBS-T), then probed using primary antibody for phospho-JNK and phospho-ERK1/2 (rabbit polyclonal, 1:1000; Cell Signaling Technology) or Olig2 (N-17) (1:50; Santa Cruz Biotechnologies) O/N at 4°C. After washing in TBS-T, the membranes were incubated with horseradish peroxidase-conjugated anti-rabbit IgG (1:3000; Pierce, Biotechnology, Rockford, IL, USA) or anti-goat IgG (1:3000; Santa Cruz Biotechnologies) and proteins were visualized using chemiluminescence (ECL, Pierce Biotechnology, Rockford, IL, USA). In order to normalize the values of phospho-JNK, phospho-ERK1/2 and Olig2, we detected β-actin in the same analysis. Membranes were stripped by strong agitation with 0.2 N NaOH (10 min, room temperature), blocked in blocking buffer for 1 h at room temperature and probed for 2 h at room temperature with anti β-actin antibody (1:5000; Sigma, St Louis, MO, USA). Afterwards membranes were incubated with horseradish peroxidase-conjugated anti-rabbit IgG (1:7500; Pierce, Biotechnology, Rockford, IL, USA) and developed as above. The bands were acquired as TIFF files and the densitometric analysis of the bands was quantified by Image J system software (NIH, Bethesda, MD, USA). Phospho-JNK, phospho-ERK1/2 and Olig2 values were expressed as percentage of β-actin run in the same Western blot analysis.

Striatal nuclear fraction

Nuclear fraction from the striatum of vehicle-treated rats ($n = 3$) was prepared according to the method of Giufrida *et al*. (1975). Briefly, striata were immersed in five volumes of ice-cold 0.3 M sucrose solution containing 1 mM K-phosphate pH 6.4, 3 mM $MgCl_2$ and protease inhibitors (buffer I), diced using a pair of scissors before being homogenized in a Dounce homogenizer (60 strokes). The homogenate was then gravity filtered through a 110-mesh nylon bolting cloth. The filtered homogenate was centrifuged at 850 × *g* for 10 min at 4°C. The pellet was used for nucleus isolation. After washing with buffer I, the pellet was resuspended in 2.4 M sucrose solution containing 1 mM K-phosphate pH 6.4 and 1 mM $MgCl_2$ and spun at 75 000 × *g* for 60 min at 4°C. The nuclear-rich fraction was resuspended in 0.3 M sucrose solution containing 1 mM K-phosphate pH 6.4 and 1 mM $MgCl_2$. The protein equivalent of 50 mg was subjected to SDS-PAGE followed by Western blot analysis as described above. Membranes were incubated overnight at 4°C with the following primary antibodies: mouse monoclonal anti-histone H1 (1:1000; Abcam, Cambridge, UK), mouse monoclonal anti MAG (1:200; Chemicon International), goat polyclonal anti Olig2 (1:200; Santa Cruz Biotechnologies) and rabbit polyclonal anti phospho-JNK (1:1000, Cell Signaling Technology). After washing in TBS-T, the membranes were incubated with the respective horseradish peroxidase-conjugated antibodies: anti-rabbit IgG (1:3000; Pierce, Biotechnology, Rockford, IL), anti-mouse (1:3000; Pierce, Biotechnology, Rockford, IL, USA) or anti-goat IgG (1:3000; Santa Cruz Biotechnologies). Proteins were visualized as described above. The bands were acquired as TIFF files and the densitometric analysis of the bands was quantified by Image J system software (NIH, Bethesda, MD). Phospho-JNK and Olig2 were normalized by an aspecific protein dye (Ponceau).

The purity of nuclear fraction was assessed by the presence of the band corresponding to histone H1 and the absence of the band corresponding to MAG. Histone that labelled nuclear-associated proteins was localized in the nuclear fraction, while MAG was localized in the extra-nuclear fraction.

Statistical analyses

Statistically significant differences in the neurological scores among vehicle-treated, SCH 58261-treated and sham-operated rats were evaluated by one-way ANOVA, followed by Newman–Keuls multiple comparison test. Statistically significant differences in brain damage, in turning behaviour and in Olig2 expression between vehicle-treated and SCH 58261-treated rats were evaluated by unpaired Student's *t*-test. Statistically significant differences in phospho-JNK and phospho-ERK1/2 levels among vehicle-treated, SCH 58261-treated and sham-operated rats were evaluated by one-way ANOVA followed by Bonferroni test.

Differences at $P < 0.05$ were considered to be statistically significant.

Results

Neuroprotective effects of SCH 58261 on turning behaviour, neurological deficit and ischaemic brain damage

SCH 58261, administered subchronically 5 min, 6 and 20 h after MCAo, blocked an acute behavioural response, turning behaviour, and reduced the neurological deficit and ischaemic brain damage evaluated 24 h after occlusion, in agreement with our previous data (Melani *et al*., 2006). One hour after MCAo, rats engaged in turning behaviour towards the side contralateral to the ischaemic hemisphere. This acute behavioural response lasted for several hours, but was no longer evident 24 h after ischaemia. Turning behaviour, expressed as mean rotations per hour, was 788.33 ± 178.01 in MCAo vehicle-treated rats ($n = 13$) and 116.92 ± 34.56 in MCAo SCH 58261-treated rats ($n = 14$). Subchronically administered SCH 58261 blocked this behaviour in a statistically significant manner (unpaired Student's *t*-test: $P < 0.0012$ vs vehicle-treated rats). Sham-operated rats ($n = 12$) did not show any turning behaviour. Turning behaviour after permanent intraluminal MCAo is a precocious index of neurological deficit and neuronal damage (Melani *et al*., 2003).

The neurological deficit and ischaemic striatal and cortical damage of vehicle-treated, SCH 58261-treated and sham-operated rats, evaluated 24 h after MCAo, are reported in Table 1. Subchronically administered SCH 58261 significantly improved the neurological deficit by 18.1% in comparison to vehicle-treated rats and reduced both cortical and striatal damage by 27.2 and 46.6%, respectively, in comparison to vehicle-treated rats. No damage was found in the sham-operated rats or in the hemisphere contralateral to the ischaemic side.

SCH 58261 reduces JNK MAPK activation in striatal *fascicula* of ischaemic hemisphere

In ischaemic vehicle-treated rats, 24 h after MCAo, activation of JNK increased within the white matter *fascicula* of the ventral caudate-putamen in structures that have features similar to fibres running parallel to each other (Fig. 1B). Some phospho-JNK immunoreactivity was also detected in the corpus callosum (data not shown). No detection of phospho-JNK was observed in the ischaemic cortex and in the contralateral hemisphere. No detection of phospho-JNK was detected in sham-operated rats either (Fig. 1A). SCH 58261 reduced phospho-JNK immunoreactivity in comparison to vehicle-treated rats (Fig. 1C).

Quantification of the two phospho-JNK isoforms (54 and 46 kDa) was performed by immunoblot analysis in the ischaemic striatum of vehicle-treated, SCH 58261-treated and sham-operated rats 24 h after MCAo (Fig. 1D). MCAo increased JNK54 isoform activation by 145% and JNK46 by 273% compared to sham-operated rats. In the ischaemic striatum, SCH 58261 caused a statistically significant reduction in both phospho-JNK isoforms: phospho-JNK54 by 81% and phospho-JNK46 by 60%, in comparison to MCAo vehicle-treated rats. The representative gels of each rat group are shown in Fig. 1E.

Table 1 Effect of SCH 58261 (0.01 mg/kg, i.p. 5 min, 6 and 20 h after occlusion) on neurological score and ischaemic brain damage evaluated 24 h after permanent MCAo

Treatment	Neurological score	Cortical damage (mm^3)	Striatal damage (mm^3)
Vehicle	$9.12 \pm 0.34^{*,\#}$	56.04 ± 3.82	25.12 ± 2.87
SCH 58261	$10.77 \pm 0.38^{\S}$	$40.81 \pm 2.65^{\dagger}$	$13.41 \pm 2.07^{\%}$
Sham-operated	17.60 ± 0.15	0	0

Data are the mean ± SE of '*n*' rats (neurological score, $n = 12$–14; brain damage, $n = 4$–5). The volume of the ipsilateral hemisphere was (mean ± SE): 132.08 ± 4.89 mm^3 in vehicle- and 128.05 ± 4.85 mm^3 in SCH 58261-treated rats. One-way ANOVA followed by Newman–Keuls multiple comparison test: $^{*}P < 0.01$ versus SCH 58261-treated rats; $^{\#,\S}P < 0.001$ versus sham-operated rats. Unpaired Student's *t*-test. $^{\dagger}P < 0.02$ and $^{\%}P < 0.014$ versus vehicle-treated rats.

MCAo induces JNK MAPK activation in oligodendrocytes of ischaemic hemisphere

To identify the cell type where JNK is activated, double immunofluorescence staining was used (Fig. 2). Figure 2C (yellow–orange colour) shows that by using Olig2 antibody directed against oligodendrocyte transcription factors, a definite co-localization between phospho-JNK (Fig. 2A, green) and oligodendrocytes (Fig. 2B, red) was found in the ventral striatum. Phospho-JNK immunoreactivity was distributed in the cell body of oligodendrocytes. Olig2 positive cells were also detected in the dorsal striatum but they did not express phospho-JNK. (not shown). Olig2 was faintly detectable in sham-operated animals (not shown).

Figure 2D shows that phospho-JNK positive cells are present only in white matter *fascicula* of the caudate-putamen and that neurons (NeuN-immunopositive cells, Fig. 2E, red) are present around white matter *fascicula*. Phospho-JNK was stained in a few scattered neurons (see arrow in Fig. 2F). Phospho-JNK positive cells are localized inside striatal white matter *fascicula* (Fig. 2G). They do not co-localize with astrocytes (Fig. 2H, GFAP-immunoreactive cells) which are localized around striatal white matter *fascicula* (Fig. 2I).

Figure 3C shows that the anti-MAG staining (Fig. 3B, red), which stains the myelin sheath, did not co-localize with phospho-JNK immunoreactivity (Fig. 3A, green), but lay in the proximity of phospho-JNK staining. Similarly, Fig. 3F shows that the anti-MAG staining (Fig. 3E, red) did not co-localize with Olig2 immunoreactivity (Fig. 3D, green) that is directed against oligodendrocyte transcription factors within the white matter *fascicula* of the caudate-putamen.

With the aim of localizing Olig2 and phospho-JNK in nuclear and extra-nuclear fractions, immunoblot analysis was performed in the ischaemic striatum of vehicle-treated rats ($n = 3$), 24 h after MCAo. Phospho-JNK extra-nuclear fraction was 1.5-fold the nuclear fraction (10.07 ± 2.97 vs 6.71 ± 0.49 values were obtained by averaging the sum of the two phosphorylated isoforms

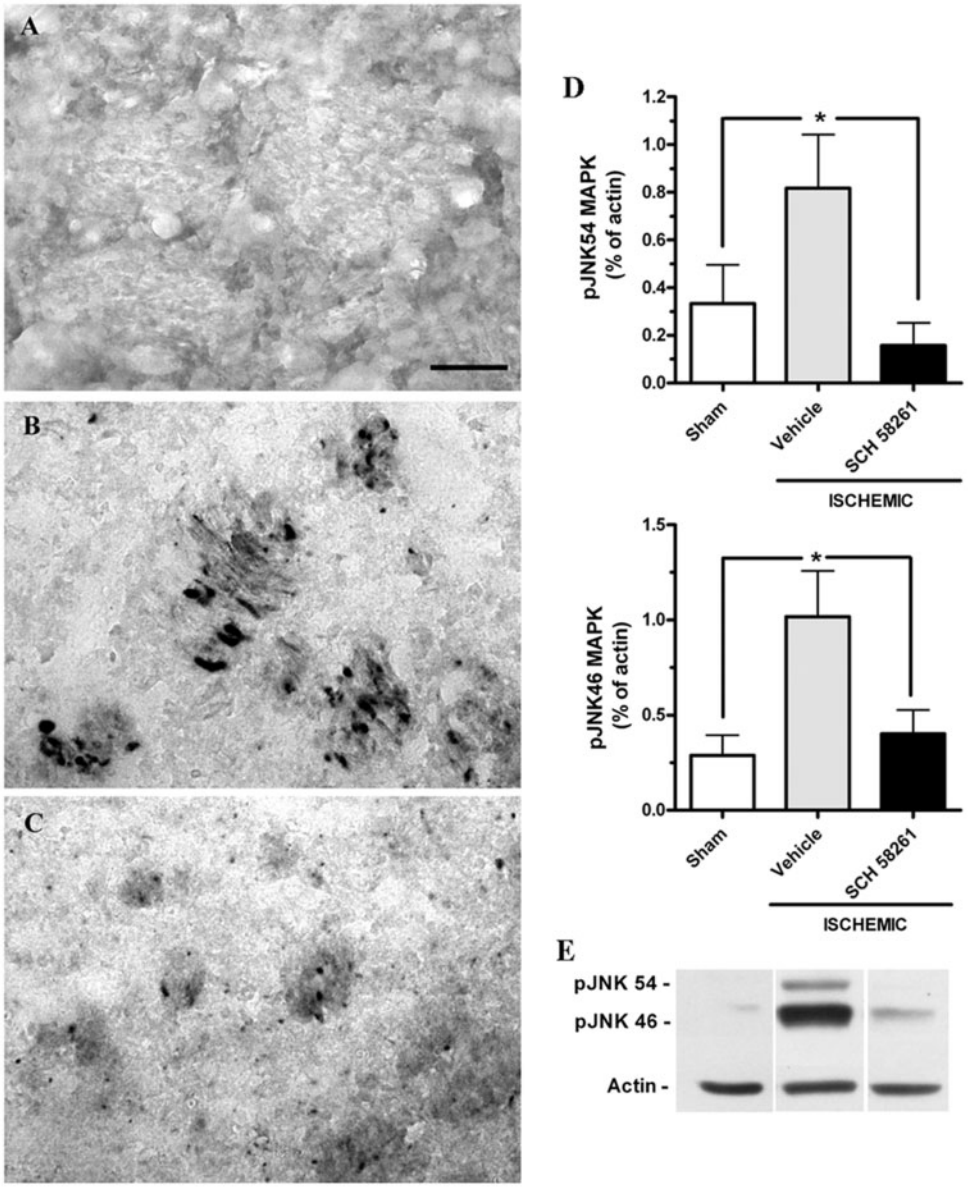

Figure 1 Effect of the selective adenosine A_{2A} receptor antagonist SCH 58261 on JNK activation in the ischaemic striatum 24 h after MCAo. (**A–C**) Representative photomicrographs of phospho-JNK immunoreactivity within white matter *fascicula* of the striatum in the occluded side of sham-operated (**A**), vehicle-treated (**B**) and SCH 58261-treated (**C**) rats. Scale bar (**A–C**): 50 μm. (**D**) Immunoblot analysis of JNK54 and JNK46 activation in the ischaemic striatum of sham-operated ($n = 5$), vehicle-treated ($n = 5$), SCH 58261-treated ($n = 5$) rats 24 h after MCAo. Phospho-JNK levels are expressed as means ± SEM of '*n*' animals in each group, normalized by control protein (β-actin). Statistical analysis by one-way ANOVA: $^*P < 0.05$ vs sham and SCH 58261 values. (**E**) Representative phospho-JNK and actin gel of sham-, vehicle- and SCH 58261-treated rats in ischaemic striatum.

normalized by an aspecific protein dye). Olig2 extra-nuclear fraction was 2.5-fold the nuclear fraction (4.43 ± 1.33 vs 1.79 ± 0.54 values normalized by an aspecific protein dye).

SCH 58261 restores myelin distribution and reduces Olig2 expression in the ischaemic hemisphere

Myelin distribution in the ischaemic area was studied by an antibody against MAG. Figure 4 shows the MAG immunostaining in the striatum of sham-operated (Fig. 4A), vehicle-treated (Fig. 4B) and SCH 58261-treated (Fig. 4C) rats. In sham-operated rats (Fig. 4A), MAG labelling is well organized within the white matter *fascicula* of the caudate-putamen. The same distribution of MAG labelling appeared in the contralateral non-ischaemic hemisphere (data not shown). In vehicle-treated rats (Fig. 4B), MAG labelling is not characterized by the typical profile of the white matter *fascicula* but appears irregularly distributed around the *fascicula*. In SCH 58261-treated rats (Fig. 4C), MAG staining appears similar to that observed in sham-operated rats.

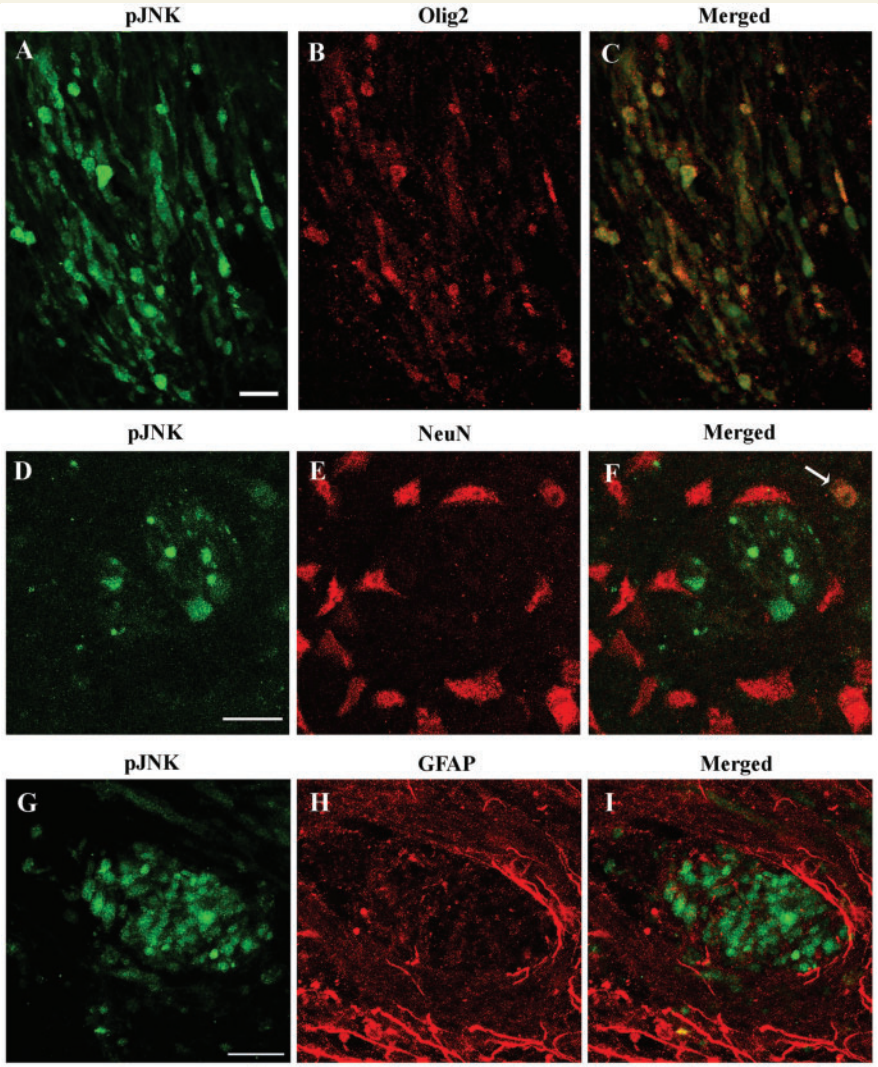

Figure 2 Double immunofluorescence was used to characterize the localization of phospho-JNK in oligodendrocytes of the ischaemic striatum 24 h after MCAo. Phospho-JNK-immunoreactive cells (pJNK, in green with fluorescein) (**A**) and Olig2-immunopositive oligodendrocytes (in red with Texas red) (**B**) showed a total co-localization (**C**) within white matter *fascicula* of the ischaemic striatum. Phospho-JNK-immunoreactive cells (**D**) and NeuN-immunopositive neurons (**E**) co-localized only in a neuron (**F**, see arrow) around the *fascicula* of the ischaemic striatum. Phospho-JNK-immunoreactive cells (**G**) and GFAP-immunopositive astrocytes (**H**) did not show co-localization (**I**). The images were obtained from serial laser confocal microscopy scans through the depth of the slice. The images were reconstructed by stacking z-step scans (1.3 μm each) which were then flattened onto one plane (**A–I**: 9 z-step scans). Scale bar (**A–I**) = 20 μm.

Olig2 expression in the white matter *fascicula* of the caudate-putamen appeared reduced in SCH-58261-treated rats (Fig. 5B) in comparison with vehicle-treated rats (Fig. 5A). The quantitative immunoblot analysis confirmed that Olig2 expression in the ischaemic striatum was significantly reduced in SCH 58261-treated rats (Fig. 5C). The representative gels of each rat group are shown in Fig. 5D.

SCH 58261 does not modify ERK1/2 MAPK activation in ischaemic hemisphere

Phospho-ERK1/2 immunoreactive cells, with morphological features of neurons, were present in the striatum (Fig. 6A) and frontoparietal cortex of sham-operated rats (Fig. 6B). While there were few phospho-ERK1/2 positive cells in the striatum and scattered throughout the structure, they were numerous and distributed in layers in the cortex.

In the ischaemic hemisphere (Fig. 6C, D), 24 h after MCAo, phospho-ERK1/2-immunoreactivity was mainly detected in cells with morphological features of glial cells and occasionally in cells with neuronal features. In the ischaemic striatum, phospho-ERK1/2 positive cells were localized around the striatal white matter *fascicula* (Fig. 6C). Ischaemia-induced ERK1/2 activation both in the striatum and cortex were not modified by treatment with SCH 58261 (Fig. 6E and F). Quantification of ERK1/2 activation was performed by immunoblot analysis on ischaemic striatum and cortex homogenates (Fig. 6G) of vehicle-treated,

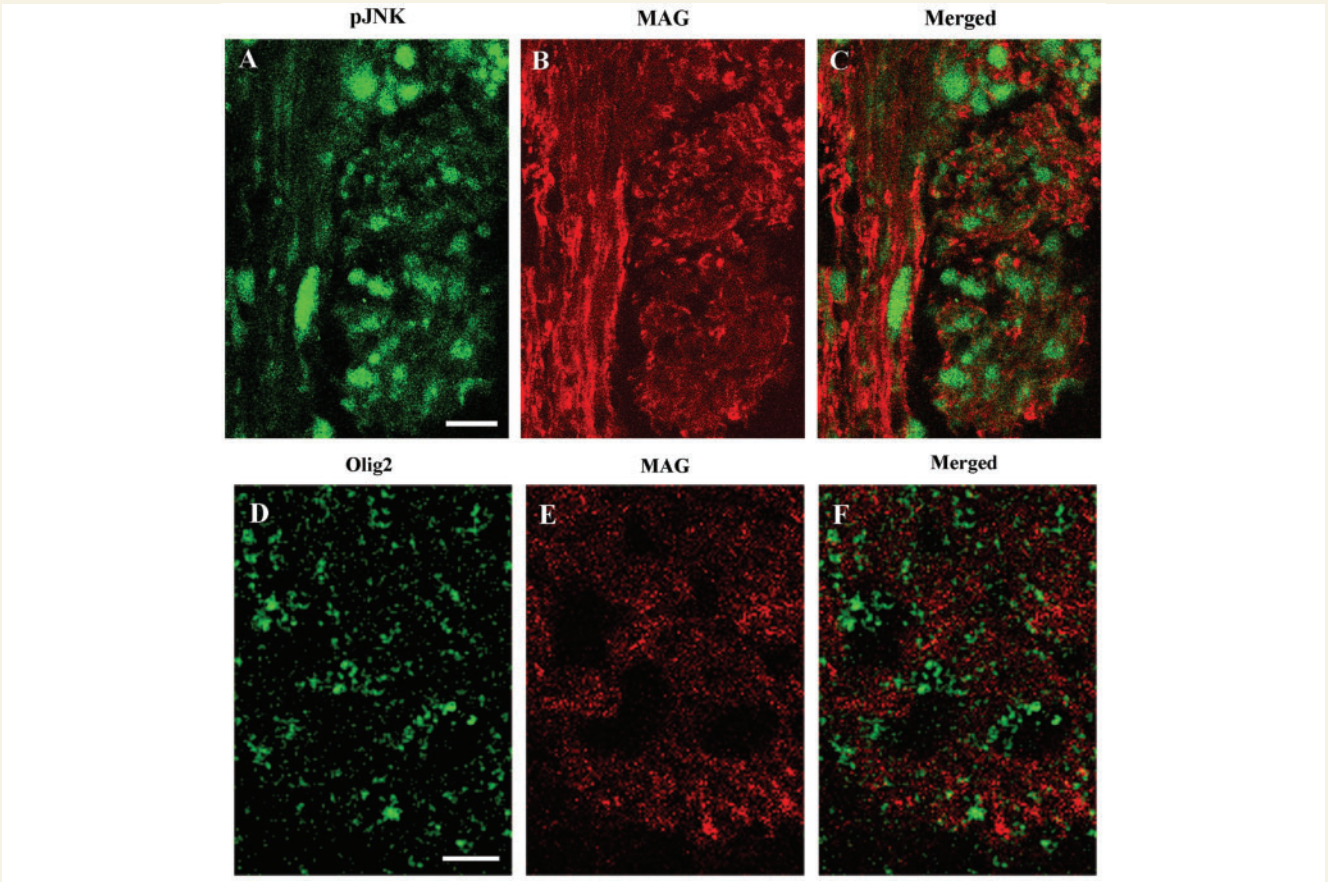

Figure 3 Phospho-JNK-immunoreactive cells (pJNK, in green with fluorescein) (**A**) and MAG-immunoreactivity (in red with Texas red) (**B**) showed a close association (**C**) but not co-localization within white matter *fascicula* of the ischaemic striatum, indicating that these antibodies label different elements of the same cell. Similarly Olig2-immunopositive oligodendrocytes (in green with fluorescein) (**D**) and MAG-immunoreactivity (in red with Texas red) (**E**) do not co-localize (**F**). The images were obtained from serial laser confocal microscopy scans through the depth of the slice. The images were reconstructed by stacking z-step scans (1.3 μm each) which were then flattened onto one plane (**A–C**: 1 z-step scans; **D–F**: 3 z-step scans). Scale bar (**A–F**) = 10 μm.

SCH 58261-treated and sham-operated rats 24 h after MCAo. Quantitative analysis was performed separately on the two phospho-ERK isoforms of apparent molecular weights of 42 and 44 kDa, respectively. MCAo caused a 30-fold increase in ERK44 and a 3-fold increase in ERK42 in the ischaemic striatum of vehicle-treated rats compared to sham-operated rats. SCH 58261 did not significantly decrease either ERK isoform activation (Fig. 6G). In the cortex of sham-operated rats ERK44 and ERK42 were significantly more activated than in the striatum (Fig. 6G). MCAo caused a 51% reduction in ERK44 and 56% reduction in ERK42 activation compared to sham-operated rats. SCH 58261 did not modify activation of ERK1/2 compared to vehicle-treated rats (Fig. 6G). Representative gels of each rat group are shown in Fig. 6H.

Twenty-four hours after MCAo, activation of ERK1/2 did not differ between vehicle-treated and SCH 58261-treated rats in either the striatum (Fig. 7A and C) or the frontoparietal cortex (Fig. 7B and D) of the contralateral, non-occluded hemisphere. Phospho-ERK1/2 was distributed mainly in the cell body and in neuronal dendrites, as demonstrated by the strict co-localization (Fig. 7G) between phospho-ERK1/2 (Fig. 7E) and NeuN- (Fig. 7F) positive cells. Quantification of the two phospho-ERK1/2 isoforms was performed by immunoblot analysis, in the contralateral striatum and cortex (Fig. 7H) of vehicle-treated, SCH 58261-treated and sham-operated rats 24 h after MCAo. Levels of phospho-ERK42 and phospho-ERK44 tended to increase (not statistically significant) in the striatum of vehicle-treated rats in comparison to sham-operated rats. SCH 58261 treatment did not significantly modify either ERK isoform activation compared to vehicle-treated rats both in the striatum and cortex. Representative gels of each rat group are shown in Fig. 7I.

MCAo induces ERK1/2 MAPK activation in microglia and neurons of the ischaemic hemisphere

To identify the cellular type where ERK1/2 was activated, double immunofluorescence staining was performed (Fig. 8).

A co-localization existed (Fig. 8C) between phospho-ERK1/2 (Fig. 8A) and OX-42 (Fig. 8B) positive cells in the ischaemic

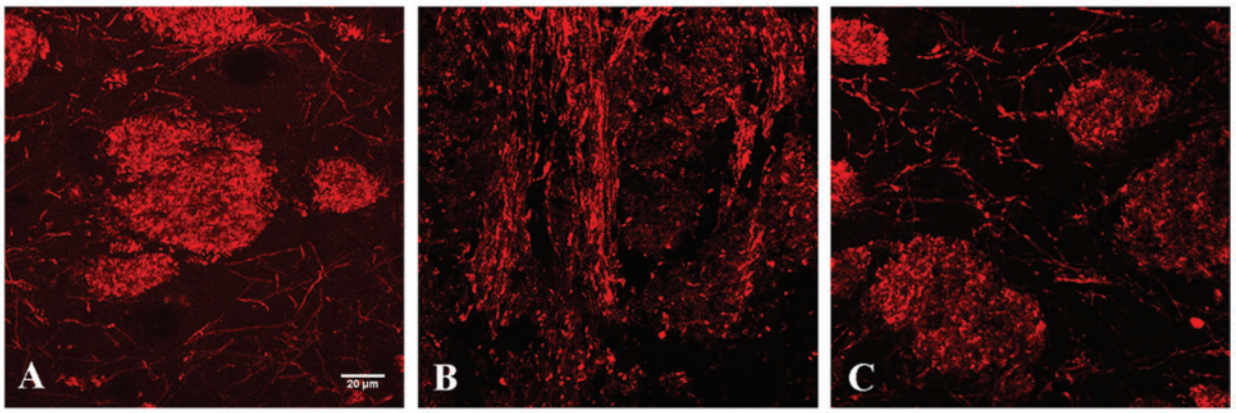

Figure 4 MAG staining in the striatum of the sham-operated rats is shown (**A**). In vehicle-treated rats, myelin redistribution is evident in the ischaemic striatal tissue (**B**). In SCH 58261-treated rats, the distribution of MAG staining is similar to that observed in sham-operated rats (**C**). Scale bar (**A–C**) = 20 µm. The images were obtained from serial laser confocal microscopy scans through the depth of the slice. The images were reconstructed by stacking z-step scans (1.3 µm each) which were then flattened onto one plane (**A–C**: 10 z-step scans).

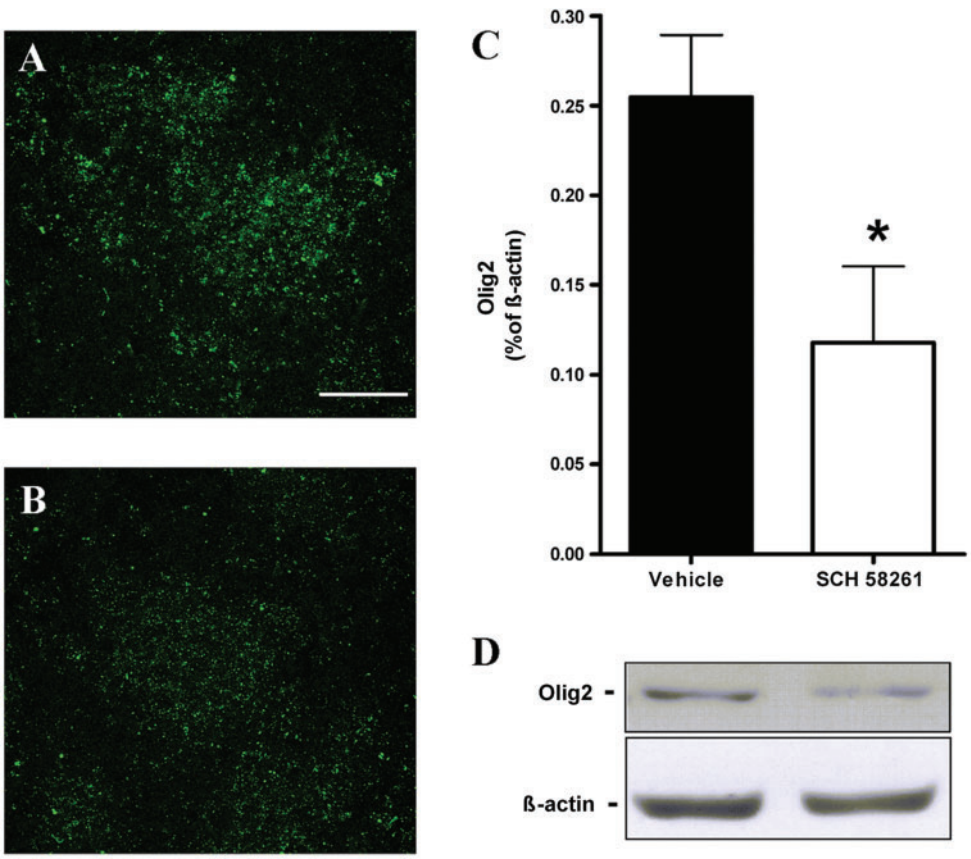

Figure 5 Olig2-immunopositive oligodendrocytes stained within white matter *fascicula* of the ischaemic striatum of vehicle-treated (**A**) and SCH 58261-treated (**B**) rats. Scale bar (**A–B**) = 40 µm. The images were obtained from serial laser confocal microscopy scans through the depth of the slice. The images were reconstructed by stacking z-step scans (1.3 µm each) and then flattened onto one plane (**A–B**: 19 z-step scans). (**C**) Immunoblot analysis of Olig2 in ischaemic striatum of vehicle-treated ($n = 5$) and SCH 58261-treated ($n = 5$) rats 24 h after MCAo. Olig2 levels are expressed as means ± SEM of 'n' animals in each group normalized by control protein (β-actin). Statistical analysis by unpaired Student's *t*-test: $^*P < 0.05$ vs vehicle-treated rats. (**D**) Representative Olig2 and β-actin gel of vehicle- and SCH 58261-treated rats in ischaemic striatum.

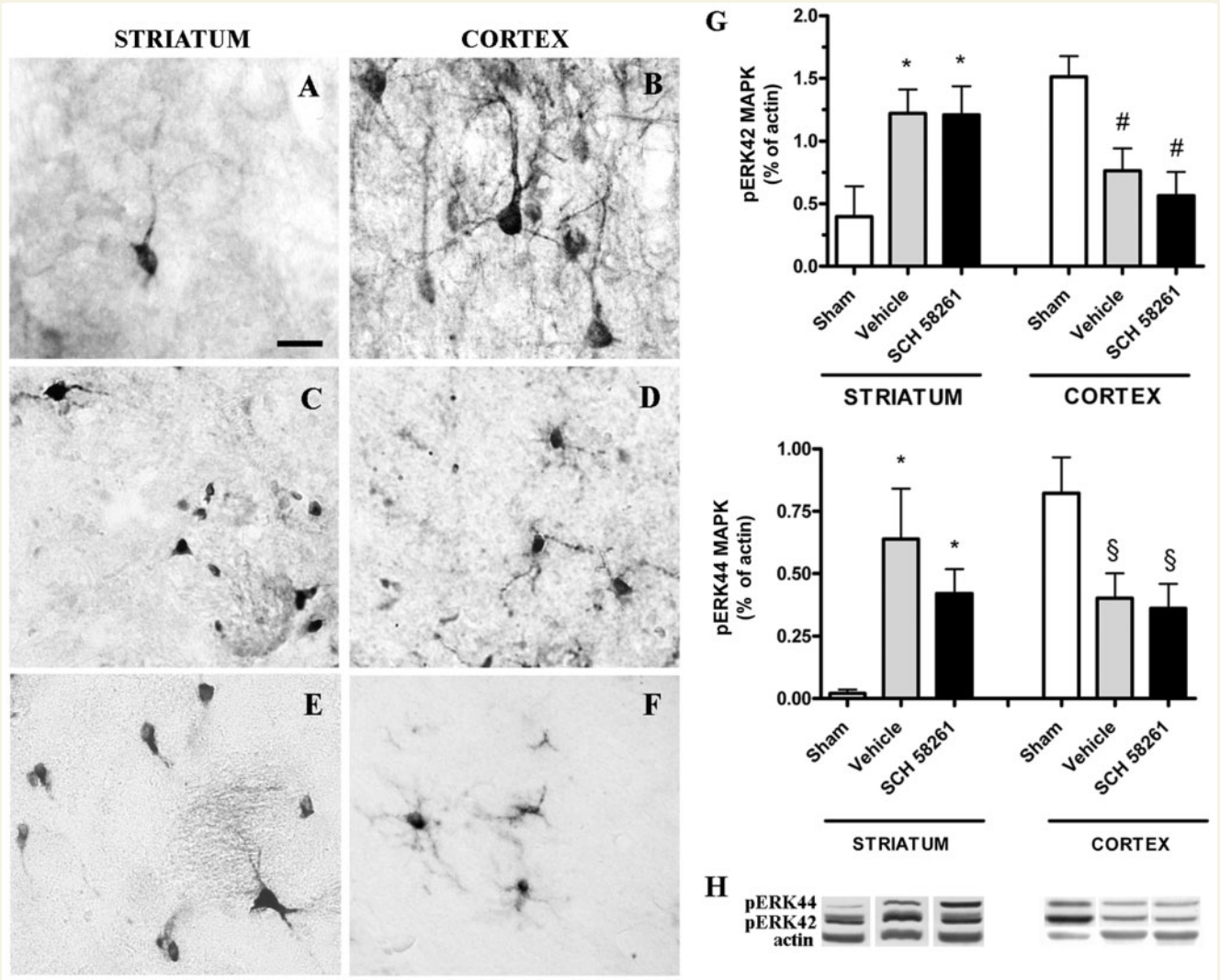

Figure 6 Effect of the selective adenosine A_{2A} receptor antagonist SCH 58261 on ERK1/2 activation in the ischaemic striatum and cortex 24 h after MCAo. (**A–F**) Representative photomicrographs of phospho-ERK1/2 positive cells in the ischaemic striatum and cortex of sham-operated (**A, B**), vehicle-treated (**C, D**) and SCH 58261-treated (**E, F**) rats. Scale bar (**A–F**): 25 μm. (**G**) Immunoblot analysis of ERK44 and ERK42 activation in the ischaemic striatum and cortex of sham-operated ($n = 5$), vehicle-treated ($n = 5$) and SCH 58261-treated ($n = 5$) rats 24 h after MCAo. Phospho-ERK42/44 levels are expressed as means ± SEM of 'n' animals in each group normalized by control protein (β-actin). Statistical analysis by one-way ANOVA: $^{*}P < 0.05$ vs sham value; $^{\#}P < 0.001$ vs sham value; $^{\S}P < 0.05$ vs sham value. (**H**) Representative phospho-ERK42/44 and actin gel of sham-, vehicle- and SCH 58261-treated rats in ischaemic striatum and cortex.

hemisphere. Phospho-ERK1/2 immunoreactivity was distributed in the cell body and processes of microglial cells which show morphological features of reactive cells.

A co-localization existed (Fig. 8F, see arrows) between phospho-ERK1/2 (Fig. 8D) and some NeuN- (Fig. 8E) positive cells in the ischaemic hemisphere.

No co-localization existed (Fig. 8I) between phospho-ERK1/2 positive cells (Fig. 8G) and GFAP-immunopositive cells (Fig. 8H) in the ischaemic tissue. Co-localization between phospho-ERK1/2 positive cells and astrocytes was found only around the blood vessels of the ischaemic hemisphere (insets of Fig. 8G–I).

Discussion

In this article, we report that JNK MAPK is definitely activated in the ischaemic striatum 24 h after MCAo and that the selective A_{2A} receptor antagonist SCH 58261 is protective against neurological deficit, brain damage and activation of JNK. We report, for the first time, that after cerebral ischaemia, oligodendrocytes strongly express the Olig2 transcription factor and that JNK is activated mainly in oligodendrocytes located in the ventral white matter *fascicula* of the caudate-putamen and in a minority of neurons of the ischaemic striatum. The A_{2A} antagonist does not affect ERK1/2 activation.

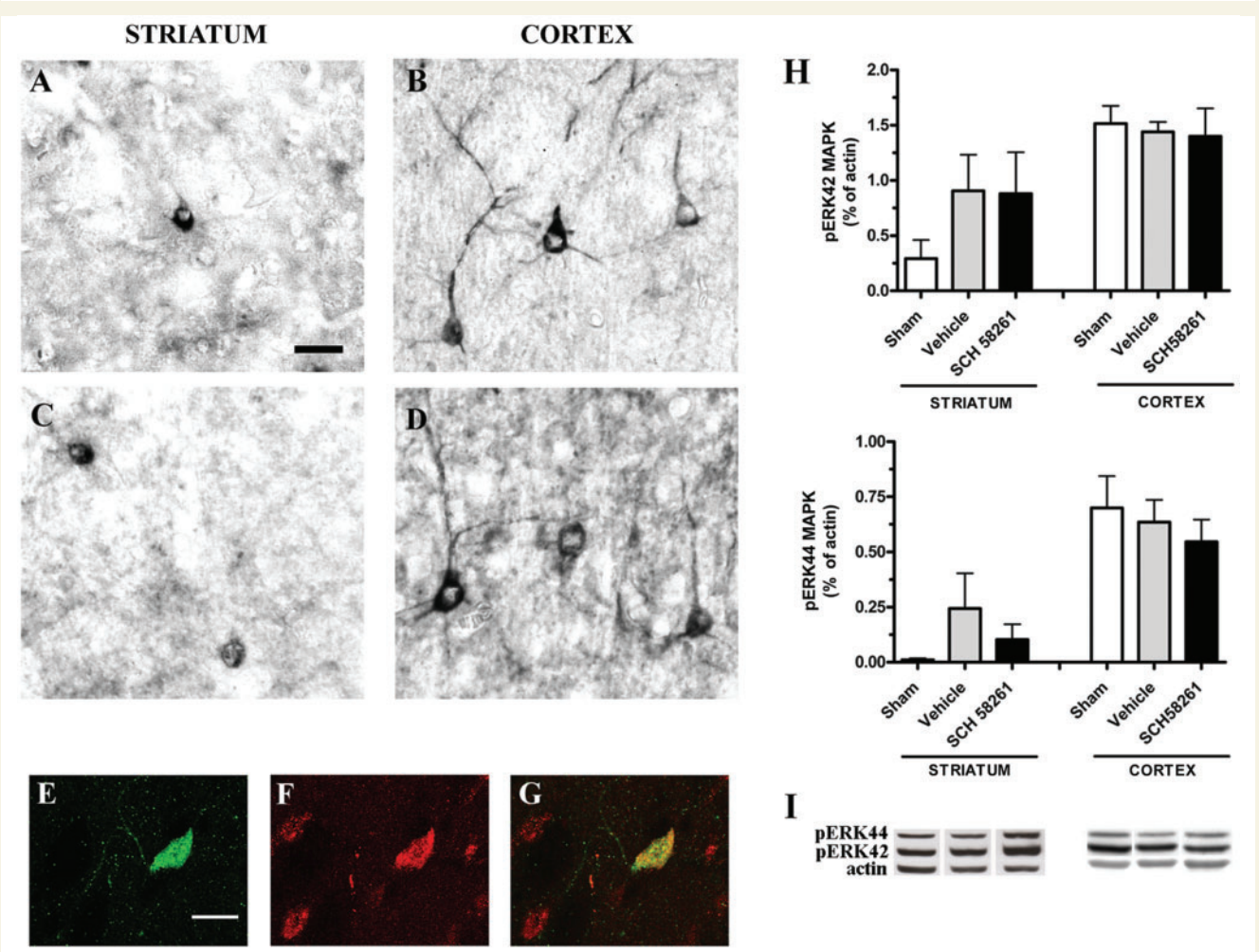

Figure 7 Phospho-ERK1/2 immunopositive neurons in the non-occluded contralateral hemisphere 24 h after MCAo. (**A–D**) Representative photomicrographs of phospho-ERK1/2 immunoreactive cells in the contralateral striatum and cortex of vehicle-treated (**A**, **B**) and SCH 58261-treated (**C**, **D**) rats. Scale bar = 25 μm. (**E–G**) Double immunofluorescence was used to characterize the localization of phospho-ERK1/2 (p-ERK, in green with fluorescein) in neurons (in red with Texas red). Phospho-ERK1/2-immunoreactive cells (**E**) and NeuN-immunopositive neurons (**F**) co-localized (**G**). The images were obtained from serial laser confocal microscopy scans through the depth of the slice. The images were reconstructed by six stacking z-step scans (1.3 μm each) and then flattened onto one plane. Scale bar = 20 μm. (**H**) Immunoblot analysis of ERK44 and ERK42 activation in the non-occluded contralateral striatum and cortex of sham-operated ($n = 5$), vehicle-treated ($n = 5$) and SCH 58261-treated ($n = 5$) rats 24 h after MCAo. Phospho-ERK42/44 levels are expressed as means ± SEM of 'n' animals in each group normalized by control protein (actin). (**I**) Representative phospho-ERK42/44 and actin gel of sham-, vehicle- and SCH 58261-treated rats in contralateral striatum and cortex.

Olig2 immunoreactivity is increased after MCAo in the ischaemic striatum

Olig2 is a transcription factor that regulates the phenotype specification of cells of oligodendroglial lineage (Lu *et al*., 2000; Zhou *et al*., 2000). The antibody to Olig2 immunolabels both developing oligodendrocyte progenitor cells and mature oligodendrocytes (Ligon *et al*., 2004; Shintaku and Yutani, 2004; Yokoo *et al*., 2004; Kuhlmann *et al*., 2008), and is currently one of the most reliable immunohistochemical markers of oligodendrocytes. Our study demonstrates the presence of Olig2 not only in the nuclear but also in the extra-nuclear fraction. Interestingly, a translocation of the Olig2 transcription factor into cytoplasm early after brain wound injury was recently reported (Magnus *et al*., 2007).

Oligodendrocytes are now known to be quite vulnerable to ischaemic stress (Shibata *et al*., 2000; Tanaka *et al*., 2001, 2003; Dewar *et al*., 2003). A widespread injury to oligodendrocytes with formation of spaces between myelin sheaths and axolemma was reported as early as 3 h after MCAo, before the appearance of necrotic neurons (Pantoni *et al*., 1996) and after chronic brain hypoperfusion (Hattori *et al*., 1992). Rapid alteration of tau was reported in oligodendrocytes after focal ischaemic injury (Irving *et al*., 1997). Therefore, oligodendrocytes and myelinated fibres appear to be extremely sensitive to ischaemic insults which result in early alteration of the subcortical white matter (Pantoni, 1998).

Mature oligodendrocytes elaborate the axonal myelin sheath (Bunge, 1968) and then play an important role in axonal

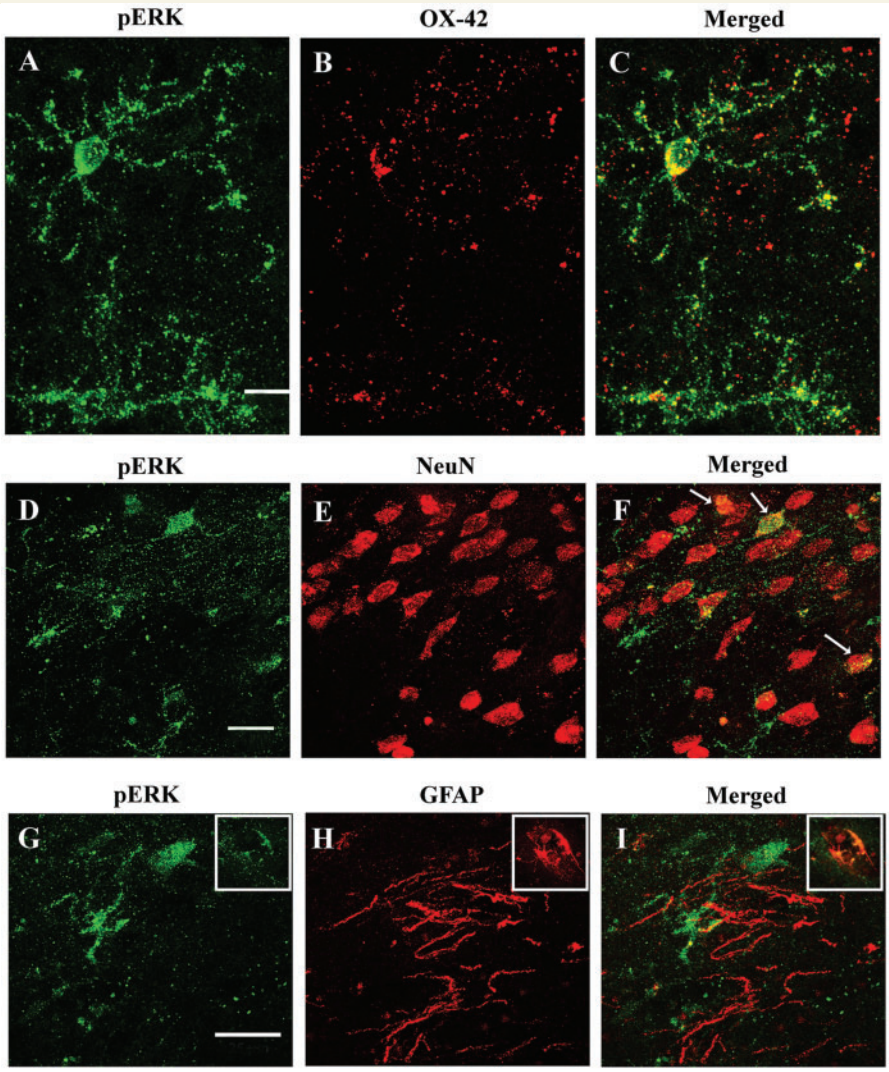

Figure 8 Phospho-ERK1/2 was identified in microglia and in a few neurons of the ischaemic hemisphere 24 h after MCAo. Double immunofluorescence was used to characterize the localization of phospho-ERK1/2 (pERK, in green with fluorescein) in microglia, neurons and astrocytes (in red with Texas red). Phospho-ERK-immunoreactive cells (**A**) and OX-42 immunopositive microglia (**B**) showed total co-localization (**C**). Phospho-ERK-immunoreactive cells (**D**) and NeuN-immunopositive neurons (**E**) showed partial co-localization (**F**, see arrows). Phospho-ERK-immunoreactive cells (**G**) and GFAP-immunopositive astrocytes (**H**) did not co-localize (**I**). The insets in **G–I** show phospho-ERK1/2 positive astrocytes around a blood vessel. The images were obtained from serial laser confocal microscopy scans through the depth of the slice. The images were reconstructed by ten stacking z-step scans (1.3 μm each) which were then flattened onto one plane. Scale bar = 10 μm (**A–C**) and 25 μm (**D–I**).

conduction and white matter injury in stroke (Sasaki *et al*., 2007). Numerous studies show that the few surviving oligodendrocytes within a region of demyelination are not induced to divide and do not significantly contribute to remyelination (Levine *et al*., 2001) whereas adult progenitor oligodendrocytes, present throughout the normal CNS, respond with reactive changes and cell division in response to tissue damage, inflammation and demyelination (Levine, 1994; Nishiyama *et al*., 1997; Redwine and Armstrong, 1998). Olig2 expressing cells in our study were definitely immunostained in the ventral striatum, the most affected area, 24 h after MCAo, and also in the dorsal striatum. On the contrary, Olig2 expressing cells were poorly detectable in sham-operated rats. The A_{2A} antagonist-induced reduction of Olig2 expression, as detected by Western blotting, indicates a lower reactivity of striatal oligodendrocytes to ischaemia.

Phospho-JNK MAPK is increased in oligodendrocytes and the selective A_{2A} receptor antagonist SCH58261 reduces JNK MAPK activation

Phospho-JNK mainly co-localizes with Olig2 stained-cells and only with a few neurons. A substantial part of phospho-JNK appeared to have already translocated into the nucleus. The cell body labelling properties of the anti-Olig2 certainly contributed positively to

this study. The anti-MAG antibodies used in our study did not point out the co-localization of phospho-JNK and oligodendrocytes but only showed that phospho-JNK staining was adjacent to MAG staining. MAG staining predominantly described myelin sheaths in nerve fibre tracts of the striatum. Co-localization of Olig2 and phospho-JNK is particularly evident in the ventral portion of the ischaemic striatum which is the most affected area 24 h after MCAo.

For the first time, this research describes the ability of adenosine A_{2A} receptors to control JNK activation in the brain. A relation between adenosine A_{2A} receptors and JNK was recently described in the heart. Reduced activation of JNK and reactive oxygen species (ROS) has been described in cardiomyocytes of A_{2A} receptor knock-out mice as well as in A_{2A} receptor antagonist-treated mice (Ribe *et al*., 2008). We report here that the A_{2A} receptor antagonist reduces JNK activation in oligodendrocytes after focal ischaemia.

Previous works demonstrate that activation of JNK is involved in oligodendrocyte death (Howe *et al*., 2004; Jurewicz *et al*., 2006). TNF-induced death of adult human oligodendrocytes is mediated by activated JNK (Jurewicz *et al*., 2003). Activation of both JNK and NF-kB transcription was described in oligodendrocytes in multiple sclerosis lesions, where oligodendrocytes are major targets of the disease (Bonetti *et al*., 1999). Following traumatic spinal cord injury, JNK activation contributes to activation of caspase 3 and of the proapoptotic regulator DP5 in oligodendrocytes and neurons (Yin *et al*., 2005).

A specific peptide inhibitor of JNK protects against cell death induced by oxygen and glucose deprivation (OGD) *in vitro* (Hirt *et al*., 2004) and by MCAo *in vivo* (Borsello *et al*., 2003; Hirt *et al*., 2004). JNK2/3 knock-out mice are protected from damage following cerebral ischaemia (Kuan *et al*., 2003; Gelderblom *et al*., 2004). Therefore, we must assume that activation of JNK in oligodendrocytes and neurons represent a noxious event after ischaemia. A_{2A} receptors have been identified in oligodendrocytes (Stevens *et al*., 2002). The possibility must be considered that A_{2A} receptors directly control JNK activation in oligodendrocytes, however, the only evidence in mouse macrophages shows that adenosine does not modify phosphorylation of JNK (Hasko *et al*., 2000).

Oligodendroglia are extremely sensitive to glutamate receptor overactivation and ensuing oxidative stress (Matute *et al*., 1997; McDonald *et al*., 1998; Matute *et al*., 2002) as well as to cytokines and adenosine (Back, 2006). Therefore, activation of JNK after ischaemia may be an epiphenomenon consequent to oxidative stress and oxidative glutamate toxicity. Glutamate toxicity in brain cortical cultured oligodendrocytes is reduced by the pan-JNK inhibitor SP600125 (Rosin *et al*., 2004). We have previously demonstrated that adenosine A_{2A} receptor antagonists reduce glutamate outflow in the first hour after ischaemia (Melani *et al*., 2006). By reducing glutamate, A_{2A} receptor antagonists may reduce JNK activation, thus allowing better survival and/or functionality of mature myelinating oligodendrocytes, as indicated by normalization of MAG staining in the ischaemic striatum. Also, reduced JNK activation might be responsible for reduced damage to developing oligodendrocyte progenitors. By reducing phospho-JNK, the A_{2A} antagonist might also reduces Olig2 expression. This is supported by the recent observation that in spinal cord primary cultures, inhibition of the MAPK pathway activation abolishes Olig2 expression (Bilican *et al*., 2008).

In conclusion, since JNK may be crucial to cell survival and regeneration in stroke, it may represent a target for pharmacological tools aimed at improving damage after ischaemia.

Activation of ERK1/2 MAPK pathway in the ischaemic striatum and reduction in the ischaemic cortex

We report that in the cortex and striatum of sham-operated animals and in the contralateral hemisphere of ischaemic animals, ERK1/2 is activated in neurons. Interestingly, in the cortex, phospho-ERK1/2 is at a much higher level in comparison to the striatum. Twenty-four hours after MCAo, in the striatum, the ERK1/2 activation occurs mainly in cells sharing the morphological features of microglia. Unlike in the striatum, 24 h after MCAo, phospho-ERK1/2 is decreased in the ischaemic cortex and immunohistochemical results show that neuronal cells are not phospho-ERK1/2 positive, whereas some microglial cells are phospho-ERK immunoreactive but only in a few areas of the cortex, i.e. frontal and cingulated areas. In agreement with our previous data (Melani *et al*., 2006), microglial cells have the features of activated cells, 24 h after focal ischaemia. Slevin *et al*. (2000) also reported ERK1/2 activation in microglial cells after brain focal ischaemia.

In light of the distinct fates of glia and neurons after ischaemia, it is likely that the same signal might be differentially activated in different brain areas at the same time after ischaemia according to cell types expressing it. After MCAo is induced by the suture technique, in relation to collateral supply, progression of ischaemic damage first appears in the striatum and thereafter in the cortex (Garcia *et al*., 1995a; Melani *et al*., 1999). In the striatum, the poor expression of phospho-ERK1/2 in neurons of naïve sham-operated animals and, after MCAo, precocious microglial expression in comparison to the cortex, may account for the net increase in phospho-ERK1/2 as detected by Western blot.

The selective A_{2A} receptor antagonist SCH58261 does not modify ERK1/2 MAPK activation

Activation of the ERK1/2 pathway results in activation of transcriptional activity, leading to cell growth and differentiation (Boulton *et al*., 1991; Marshall, 1995; Segal and Greenberg, 1996). However, in post-mitotic cells within the central and peripheral nervous system, ERK1/2 may play additional roles. In the MCAo model, pre-treatment with inhibitors of the MEK1/ERK pathway results in protection of the brain 22–24 h after ischaemic injury, reducing both brain damage, neurological deficit (Alessandrini *et al*., 1999; Namura *et al*., 2001; Wang *et al*., 2003) and IL-1beta expression (Wang *et al*., 2004). Treatment of neuronal cultures with the specific MEK inhibitor PD-98059 reduces damage following glutamate (Bading and Greenberg, 1991) or okadic acid (Runden *et al*., 1998) exposure or

seizure-like activity (Runden *et al*., 1998), showing that activation of the ERK pathway is involved in neuronal death. This suggests that, although normally involved in cell growth and differentiation, prolonged activation of the ERK pathway in certain conditions may be detrimental to survival of neurons. A main cell location of ERK1/2 is described in neurons, although modifications of ERK1/2 activation after focal cerebral ischaemia have been reported in different spatial locations and different cell types (Irving *et al*., 2000; Wu *et al*., 2000; Borsello *et al*., 2003; Wang *et al*., 2003).

In this study, we have demonstrated that the A_{2A} receptor antagonist SCH 58261 does not modify phospho-ERK1/2. Therefore, modification of the activation of the ERK1/2 pathway does not help explain the protective effect of A_{2A} receptor antagonism that is seen 24 h after focal ischaemia.

Conclusions

These results show that protection attained 24 h after MCAo, by repeated post-ischaemic administration of A_{2A} receptor antagonists, involves reduced activation of JNK MAPK. The adenosine A_{2A} receptor antagonist reduces activation of JNK mostly in oligodendrocytes of the ischaemic striatum and protects from myelin disorganization, as demonstrated by the normalization of MAG staining in the striatum of treated rats in comparison to vehicles. Oligodendrocytes are known to be quite vulnerable to ischaemic stress before the appearance of necrotic neurons (Pantoni *et al*., 1996). Suffering probably involves both mature oligodendrocytes and adult progenitors by reducing the potential of oligodendrogenesis that might occur in response to demyelination (see Dubois-Dalcq *et al*., 2008; Nait-Oumesmar *et al*., 2008). Although, therapeutic transplantation and mobilization of endogenous precursors to repair the diseased or injured brain are still in their infancy, drug strategies aimed at overcoming the activity of glial scar inhibitory molecules that hinder myelin and neuronal reconstitution, might be valuable in the treatment of ischaemic stroke (Levine *et al*., 2001). The efficacy of A_{2A} receptor antagonism in reducing activation of JNK MAPK in oligodendrocytes suggests a mechanism of protection consisting of scarring oligodendrocyte inhibitory molecules that can hinder myelin and neuronal reconstitution.

Acknowledgements

We would like to thank Prof. Giovanni Baraldi for the generous gift of SCH 58261; Prof. Fiorella Casamenti for generously permitting use of the light microscope.

Funding

IRCCS Centro Neurolesi 'Bonino-Pulejo', Messina, Italy; Italian Ministry of Health; Fondazione Ente Cassa di Risparmio di Firenze, Italy.

References

Alessandrini A, Namura S, Moskowitz MA, Bonventre JV. MEK1 protein kinase inhibition protects against damage resulting from focal cerebral ischemia. Proc Natl Acad Sci USA 1999; 96: 12866–9.

Back SA. Perinatal white matter injury: the changing spectrum of pathology and emerging insights into pathogenetic mechanisms. Ment Retard Dev Disabil Res Rev 2006; 12: 129–40.

Bading H, Greenberg ME. Stimulation of protein tyrosine phosphorylation by NMDA receptor activation. Science 1991; 253: 912–4.

Bilican B, Fiore-Heriche C, Compston A, Allen ND, Chandran S. Induction of Olig2 precursors by FGF involves BMP signalling blockade at the Smad level. PLoS ONE 2008; 3: e2863.

Bonetti B, Stegagno C, Cannella B, Rizzuto N, Moretto G, Raine CS. Activation of NF-kappaB and c-jun transcription factors in multiple sclerosis lesions. Implications for oligodendrocyte pathology. Am J Pathol 1999; 155: 1433–8.

Borsello T, Clarke PG, Hirt L, Vercelli A, Repici M, Schorderet DF, et al. A peptide inhibitor of c-Jun N-terminal kinase protects against excitotoxicity and cerebral ischemia. Nat Med 2003; 9: 1180–6.

Boulton TG, Nye SH, Robbins DJ, Ip NY, Radziejewska E, Morgenbesser SD, et al. ERKs: a family of protein-serine/threonine kinases that are activated and tyrosine phosphorylated in response to insulin and NGF. Cell 1991; 65: 663–75.

Brambilla R, Cottini L, Fumagalli M, Ceruti S, Abbracchio MP. Blockade of A_{2A} adenosine receptors prevents basic fibroblast growth factor-induced reactive astrogliosis in rat striatal primary astrocytes. Glia 2003; 43: 190–4.

Bunge RP. Glial cells and the central myelin sheath. Physiol Rev 1968; 48: 197–251.

Chen JF, Huang Z, Ma J, Zhu J, Moratalla R, Standaert D, et al. A_{2A} adenosine receptor deficiency attenuates brain injury induced by transient focal ischemia in mice. J Neurosci 1999; 19: 9192–200.

Chen JF, Pedata F. Modulation of ischemic brain injury and neuroinflammation by adenosine A_{2A} receptors. Curr Pharm Des 2008; 14: 1490–9.

Chen JF, Sonsalla PK, Pedata F, Melani A, Domenici MR, Popoli P, et al. Adenosine A_{2A} receptors and brain injury: broad spectrum of neuroprotection, multifaceted actions and 'fine tuning' modulation. Prog Neurobiol 2007; 83: 310–31.

Dewar D, Underhill SM, Goldberg MP. Oligodendrocytes and ischemic brain injury. J Cereb Blood Flow Metab 2003; 23: 263–74.

Dubois-Dalcq M, Williams A, Stadelmann C, Stankoff B, Zalc B, Lubetzki C. From fish to man: understanding endogenous remyelination in central nervous system demyelinating diseases. Brain 2008; 131: 1686–700.

Esneault E, Castagne V, Moser P, Bonny C, Bernaudin M. D-JNKi, a peptide inhibitor of c-Jun N-terminal kinase, promotes functional recovery after transient focal cerebral ischemia in rats. Neuroscience 2008; 152: 308–20.

Fiebich BL, Biber K, Lieb K, van Calker D, Berger M, Bauer J, et al. Cyclooxygenase-2 expression in rat microglia is induced by adenosine A_{2A}-receptors. Glia 1996; 18: 152–60.

Fink JS, Weaver DR, Rivkees SA, Peterfreund RA, Pollack AE, Adler EM, et al. Molecular cloning of the rat A_2 adenosine receptor: selective co-expression with D2 dopamine receptors in rat striatum. Brain Res Mol Brain Res 1992; 14: 186–95.

Garcia JH, Liu KF, Ho KL. Neuronal necrosis after middle cerebral artery occlusion in Wistar rats progresses at different time intervals in the caudoputamen and the cortex. Stroke 1995a; 26: 636–42.

Garcia JH, Wagner S, Liu KF, Hu XJ. Neurological deficit and extent of neuronal necrosis attributable to middle cerebral artery occlusion in rats. Statistical validation. Stroke 1995b; 26: 627–34.

Gelderblom M, Eminel S, Herdegen T, Waetzig V. c-Jun N-terminal kinases (JNKs) and the cytoskeleton–functions beyond neurodegeneration. Int J Dev Neurosci 2004; 22: 559–64.

Giovannini MG. Double-label confocal microscopy of phosphorylated protein kinases involved in long-term potentiation. Methods Enzymol 2002; 345: 426–36.

Giovannini MG, Blitzer RD, Wong T, Asoma K, Tsokas P, Morrison JH, et al. Mitogen-activated protein kinase regulates early phosphorylation and delayed expression of Ca2+/calmodulin-dependent protein kinase II in long-term potentiation. J Neurosci 2001; 21: 7053–62.

Giufrida AM, Cox D, Mathias AP. RNA polymerade activity in various classes of nuclei from different regions of rat brain during postnatal development. J Neurochem 1975; 24: 749–55.

Haskó G, Kuhel DG, Chen JF, Schwarzschild MA, Deitch EA, Mabley JG, et al. Adenosine inhibits IL-12 and TNF-[alpha] production via adenosine A_{2A} receptor-dependent and independent mechanisms. FASEB J 2000; 14: 2065–74.

Hattori H, Takeda M, Kudo T, Nishimura T, Hashimoto S. Cumulative white matter changes in the gerbil brain under chronic cerebral hypoperfusion. Acta Neuropathol 1992; 84: 437–42.

Hirt L, Badaut J, Thevenet J, Granziera C, Regli L, Maurer F, et al. D-JNKI1, a cell-penetrating c-Jun-N-terminal kinase inhibitor, protects against cell death in severe cerebral ischemia. Stroke 2004; 35: 1738–43.

Howe CL, Bieber AJ, Warrington AE, Pease LR, Rodriguez M. Antiapoptotic signaling by a remyelination-promoting human antimyelin antibody. Neurobiol Dis 2004; 15: 120–31.

Irving EA, Bamford M. Role of mitogen- and stress-activated kinases in ischemic injury. J Cereb Blood Flow Metab 2002; 22: 631–47.

Irving EA, Barone FC, Reith AD, Hadingham SJ, Parsons AA. Differential activation of MAPK/ERK and p38/SAPK in neurones and glia following focal cerebral ischaemia in the rat. Brain Res Mol Brain Res 2000; 77: 65–75.

Irving EA, Yatsushiro K, McCulloch J, Dewar D. Rapid alteration of tau in oligodendrocytes after focal ischemic injury in the rat: involvement of free radicals. J Cereb Blood Flow Metab 1997; 17: 612–22.

Jurewicz A, Matysiak M, Andrzejak S, Selmaj K. TRAIL-induced death of human adult oligodendrocytes is mediated by JNK pathway. Glia 2006; 53: 158–66.

Jurewicz A, Matysiak M, Tybor K, Selmaj K. TNF-induced death of adult human oligodendrocytes is mediated by c-jun NH2-terminal kinase-3. Brain 2003; 126: 1358–70.

Kuan CY, Whitmarsh AJ, Yang DD, Liao G, Schloemer AJ, Dong C, et al. A critical role of neural-specific JNK3 for ischemic apoptosis. Proc Natl Acad Sci USA 2003; 100: 15184–9.

Kuhlmann T, Miron V, Cuo Q, Wegner C, Antel J, Bruck W. Differentiation block of oligodendroglial progenitor cells as a cause for remyelination failure in chronic multiple sclerosis. Brain 2008; 131: 1749–58.

Lee YC, Chien CL, Sun CN, Huang CL, Huang NK, Chiang MC, et al. Characterization of the rat A_{2A} adenosine receptor gene: a 4.8-kb promoter-proximal DNA fragment confers selective expression in the central nervous system. Eur J Neurosci 2003; 18: 1786–96.

Levine JM. Increased expression of the NG2 chondroitin-sulfate proteoglycan after brain injury. J Neurosci 1994; 14: 4716–30.

Levine JM, Reynolds R, Fawcett JW. The oligodendrocyte precursor cell in health and disease. Trends Neurosci 2001; 24: 39–47.

Ligon KL, Alberta JA, Kho AT, Weiss J, Kwaan MR, Nutt CL, et al. The oligodendroglial lineage marker OLIG2 is universally expressed in diffuse gliomas. J Neuropathol Exp Neurol 2004; 63: 499–509.

Longa EZ, Weinstein PR, Carlson S, Cummins R. Reversible middle cerebral artery occlusion without craniectomy in rats. Stroke 1989; 20: 84–91.

Lu QR, Yuk D, Alberta JA, Zhu Z, Pawlitzky I, Chan J, et al. Sonic hedgehog–regulated oligodendrocyte lineage genes encoding bHLH proteins in the mammalian central nervous system. Neuron 2000; 25: 317–29.

Magnus T, Coksaygan T, Korn T, Xue H, Arumugam TV, Mughal MR, et al. Evidence that nucleocytoplasmic Olig2 translocation mediates brain-injury-induced differentiation of glial precursors to astrocytes. J Neurosci Res 2007; 85: 2126–37.

Marshall CJ. Specificity of receptor tyrosine kinase signaling: transient versus sustained extracellular signal-regulated kinase activation. Cell 1995; 80: 179–85.

Matute C, Alberdi E, Ibarretxe G, Sanchez-Gomez MV. Excitotoxicity in glial cells. Eur J Pharmacol 2002; 447: 239–46.

Matute C, Sanchez-Gomez MV, Martinez-Millan L, Miledi R. Glutamate receptor-mediated toxicity in optic nerve oligodendrocytes. Proc Natl Acad Sci USA 1997; 94: 8830–5.

McDonald JW, Althomsons SP, Hyrc KL, Choi DW, Goldberg MP. Oligodendrocytes from forebrain are highly vulnerable to AMPA/kainate receptor-mediated excitotoxicity. Nat Med 1998; 4: 291–7.

Melani A, Gianfriddo M, Vannucchi MG, Cipriani S, Baraldi PG, Giovannini MG, et al. The selective A_{2A} receptor antagonist SCH 58261 protects from neurological deficit, brain damage and activation of p38 MAPK in rat focal cerebral ischemia. Brain Res 2006; 1073–4: 470–80.

Melani A, Pantoni L, Bordoni F, Gianfriddo M, Bianchi L, Vannucchi MG, et al. The selective A_{2A} receptor antagonist SCH 58261 reduces striatal transmitter outflow, turning behavior and ischemic brain damage induced by permanent focal ischemia in the rat. Brain Res 2003; 959: 243–50.

Melani A, Pantoni L, Corsi C, Bianchi L, Monopoli A, Bertorelli R, et al. Striatal outflow of adenosine, excitatory amino acids, gamma-aminobutyric acid, and taurine in awake freely moving rats after middle cerebral artery occlusion: correlations with neurological deficit and histopathological damage. Stroke 1999; 30: 2448–54.

Monopoli A, Casati C, Lozza G, Forlani A, Ongini E. Cardiovascular pharmacology of the A_{2A} adenosine receptor antagonist, SCH 58261, in the rat. J Pharmacol Exp Ther 1998a; 285: 9–15.

Monopoli A, Lozza G, Forlani A, Mattavelli A, Ongini E. Blockade of adenosine A_{2A} receptors by SCH 58261 results in neuroprotective effects in cerebral ischaemia in rats. Neuroreport 1998b; 9: 3955–9.

Nait-Oumesmar B, Picard-Riera N, Kerninon C, Baron-Van Evercooren A. The role of SVZ-derived neural precursors in demyelinating diseases: from animal models to multiple sclerosis. J Neurol Sci 2008; 265: 26–31.

Namura S, Iihara K, Takami S, Nagata I, Kikuchi H, Matsushita K, et al. Intravenous administration of MEK inhibitor U0126 affords brain protection against forebrain ischemia and focal cerebral ischemia. Proc Natl Acad Sci USA 2001; 98: 11569–74.

Nishiyama A, Yu M, Drazba JA, Tuohy VK. Normal and reactive NG2+ glial cells are distinct from resting and activated microglia. J Neurosci Res 1997; 48: 299–312.

Nishizaki T, Nagai K, Nomura T, Tada H, Kanno T, Tozaki H, et al. A new neuromodulatory pathway with a glial contribution mediated via A_{2A} adenosine receptors. Glia 2002; 39: 133–47.

Pantoni L. Experimental approaches to white matter disease. Dement Geriatr Cogn Disord 1998; 9 (Suppl 1): 20–4.

Pantoni L, Garcia JH, Gutierrez JA. Cerebral white matter is highly vulnerable to ischemia. Stroke 1996; 27: 1641–6.

Pedata F, Gianfriddo M, Turchi D, Melani A. The protective effect of adenosine A_{2A} receptor antagonism in cerebral ischemia. Neurol Res 2005; 27: 169–74.

Phillis JW. Adenosine and adenine nucleotides as regulators of cerebral blood flow: roles of acidosis, cell swelling, and KATP channels. Crit Rev Neurobiol 2004; 16: 237–70.

Redwine JM, Armstrong RC. In vivo proliferation of oligodendrocyte progenitors expressing PDGFalphaR during early remyelination. J Neurobiol 1998; 37: 413–28.

Repici M, Borsello T. JNK pathway as therapeutic target to prevent degeneration in the central nervous system. Adv Exp Med Biol 2006; 588: 145–55.

Ribé D, Sawbridge D, Thakur S, Hussey M, Ledent C, Kitchen I, et al. Adenosine A_{2A} receptor signaling regulation of cardiac NADPH oxidase activity. Free Radic Biol Med 2008; 44: 1433–42.

Rosin C, Bates TE, Skaper SD. Excitatory amino acid induced oligodendrocyte cell death in vitro: receptor-dependent and -independent mechanisms. J Neurochem 2004; 90: 1173–85.

Rosin DL, Robeva A, Woodard RL, Guyenet PG, Linden J. Immunohistochemical localization of adenosine A_{2A} receptors in the rat central nervous system. J Comp Neurol 1998; 401: 163–86.

Rundén E, Seglen PO, Haug FM, Ottersen OP, Wieloch T, Shamloo M, et al. Regional selective neuronal degeneration after protein phosphatase inhibition in hippocampal slice cultures: evidence for a MAP kinase-dependent mechanism. J Neurosci 1998; 18: 7296–305.

Sasaki M, Li B, Lankford KL, Radtke C, Kocsis JD. Remyelination of the injured spinal cord. Prog Brain Res 2007; 161: 419–33.

Schiffmann SN, Libert F, Vassart G, Vanderhaeghen JJ. Distribution of adenosine A_2 receptor mRNA in the human brain. Neurosci Lett 1991; 130: 177–81.

Segal RA, Greenberg ME. Intracellular signaling pathways activated by neurotrophic factors. Annu Rev Neurosci 1996; 19: 463–89.

Shibata M, Hisahara S, Hara H, Yamawaki T, Fukuuchi Y, Yuan J, et al. Caspases determine the vulnerability of oligodendrocytes in the ischemic brain. J Clin Invest 2000; 106: 643–53.

Shintaku M, Yutani C. Oligodendrocytes within astrocytes ('emperipolesis') in the white matter in Creutzfeldt-Jakob disease. Acta Neuropathol 2004; 108: 201–6.

Slevin M, Krupinski J, Slowik A, Rubio F, Szczudlik A, Gaffney J. Activation of MAP kinase (ERK-1/ERK-2), tyrosine kinase and VEGF in the human brain following acute ischaemic stroke. Neuroreport 2000; 11: 2759–64.

Stevens B, Porta S, Haak LL, Gallo V, Fields RD. Adenosine: a neuron-glial transmitter promoting myelination in the CNS in response to action potentials. Neuron 2002; 36: 855–68.

Tanaka K, Nogawa S, Ito D, Suzuki S, Dembo T, Kosakai A, et al. Activation of NG2-positive oligodendrocyte progenitor cells during post-ischemic reperfusion in the rat brain. Neuroreport 2001; 12: 2169–74.

Tanaka K, Nogawa S, Suzuki S, Dembo T, Kosakai A. Upregulation of oligodendrocyte progenitor cells associated with restoration of mature oligodendrocytes and myelination in peri-infarct area in the rat brain. Brain Res 2003; 989: 172–9.

Trincavelli ML, Melani A, Guidi S, Cuboni S, Cipriani S, Pedata F, et al. Regulation of A_{2A} adenosine receptor expression and functioning following permanent focal ischemia in rat brain. J Neurochem 2008; 104: 479–90.

Wang Y, Faux SP, Hallden G, Kirn DH, Houghton CE, Lemoine NR, et al. Interleukin-1beta and tumour necrosis factor-alpha promote the transformation of human immortalised mesothelial cells by erionite. Int J Oncol 2004; 25: 173–8.

Wang Z, Chen X, Zhou L, Wu D, Che X, Yang G. Effects of extracellular signal-regulated kinase (ERK) on focal cerebral ischemia. Chin Med J (Engl) 2003; 116: 1497–503.

Wittendorp MC, Boddeke HW, Biber K. Adenosine A3 receptor-induced CCL2 synthesis in cultured mouse astrocytes. Glia 2004; 46: 410–8.

Wu DC, Ye W, Che XM, Yang GY. Activation of mitogen-activated protein kinases after permanent cerebral artery occlusion in mouse brain. J Cereb Blood Flow Metab 2000; 20: 1320–30.

Yin KJ, Kim GM, Lee JM, He YY, Xu J, Hsu CY. JNK activation contributes to DP5 induction and apoptosis following traumatic spinal cord injury. Neurobiol Dis 2005; 20: 881–9.

Yokoo H, Nobusawa S, Takebayashi H, Ikenaka K, Isoda K, Kamiya M, et al. Anti-human Olig2 antibody as a useful immunohistochemical marker of normal oligodendrocytes and gliomas. Am J Pathol 2004; 164: 1717–25.

Zhou Q, Wang S, Anderson DJ. Identification of a novel family of oligodendrocyte lineage-specific basic helix-loop-helix transcription factors. Neuron 2000; 25: 331–43.